ELSEVIER

Computers and Chemistry 26 (2002) 131–140

Computers & Chemistry

www.elsevier.com/locate/compchem

Theoretical study of the morphologically originated noise associated with the transmittance of a precipitation system

J.A. Poce-Fatou *, R. Alcántara, J. Martín

Departamento de Química Física, Facultad de Ciencias, Universidad de Cádiz, Apartado de Correos 40, 11510 Puerto Real (Cádiz), Spain

Received 20 February 2001; received in revised form 21 April 2001; accepted 14 May 2001

Abstract

In this paper we present the results of a computational study that analyses the relationship between the noise associated with the optical transmittance of a system of particles and the morphology of such particles. Computational algorithms have been developed in order to represent the different morphologies within a wide range of sizes. By using this methodology, it has been possible to study the morphology of particles in a virtual system, therefore avoiding the distortions that would inevitably be present in a real system. As a consequence of this study, a classification of the morphologies observed has been made according to the amount of noise they would add to the transmittance of a system of particles. The theoretical results obtained are in good agreement with the available experimental data obtained in real systems. © 2002 Elsevier Science Ltd. All rights reserved.

Keywords: Precipitation; Noise; Transmittance; Simulation; Morphology; Polyhedron

1. Introduction

We have recently made measurements of transmittance in precipitation systems in which PbI_2, $PbSO_4$, $BaSO_4$ and BaC_2O_4 precipitates were formed by means of injecting an inducing agent into a base solution (Poce-Fatou et al., 2001a).

Transmittances were measured using a laser beam focused at the geometric centre of the precipitation cell. This type of laser beam describes a hyperbolic path and is capable of detecting particles of the same size range as its focal region. For that reason, the transmittance signal experiences significant fluctuations which are recorded as noise associated with this signal (Martín et al., 1991, 1992).

This associated noise may be caused by several factors, among which we could mention:

1. Factors which may be regarded as unconnected with the precipitation system itself. This group includes variations generated by the measuring instruments, imperfections of the experimental arrangement, infinitesimal changes in the external conditions, etc.
2. Factors related to the characteristics of the laser probe used in the experiment. Within this group we include the elements that characterise the hyperbolic path of the beam, namely the laser wavelength, the prefocussed radius of the beam, and the focal length of the lens used for focussing the beam (Gerrard and Burch, 1994; Poce-Fatou et al., 2001b).
3. Factors related to the nature of the precipitation medium, including changes of orientation and position of the particles, the presence of a variety of sizes, as well as factors related to the presence of different morphologies in the precipitation medium.

* Corresponding author. Tel.: +34-956-016-178; fax: +34-956-016-288.

E-mail address: juanantonio.poce@uca.es (J.A. Poce-Fatou).

PII: S0097-8485(01)00090-0

In connection with the last group of factors mentioned above, and with regard to the measurements of transmittance made in the course of these experiments, we have found signs that suggest some kind of relationship between the morphology of the precipitate and the noise associated with the measured signal.

In the tests carried out under identical experimental conditions and precipitated mass, the systems made up of flat particles of PbI_2 and $PbSO_4$, generated variations of transmittance whose levels of associated noise turned out to be much higher than in the case of systems made up of elongated particles of $BaSO_4$ and BaC_2O_4.

With the aim of doing an in-depth analysis of these facts and characterising the relationship between the noise associated with the transmittance of a precipitation system and the morphology of the precipitate, we have developed a theoretical study based upon computerised simulation techniques.

2. Materials and methods

2.1. The concept of morphological noise

We have recently developed an experimental arrangement for a study of precipitation systems based upon measurement of the noise associated with the transmittance (Poce-Fatou et al., 2001a). Subsequently, we have designed a computer program (PPSP), (Poce-Fatou et al., 2001b), which emulates the characteristics of such systems and extracts simulated transmittances and associated noises.

This program provides a model of a pure nucleation process in which spherical particles with a unimodal distribution of volumes precipitate. Particles intercepting the beam at some point along its path will generate projections onto a virtual photoreceptor placed orthogonally to the propagation axis. Supposing these particles absorb 100% of the incident radiation, transmittances are calculated as a value proportional to the area of the photoreceptor unit on which there is no projection (Fig. 1), according to the expression,

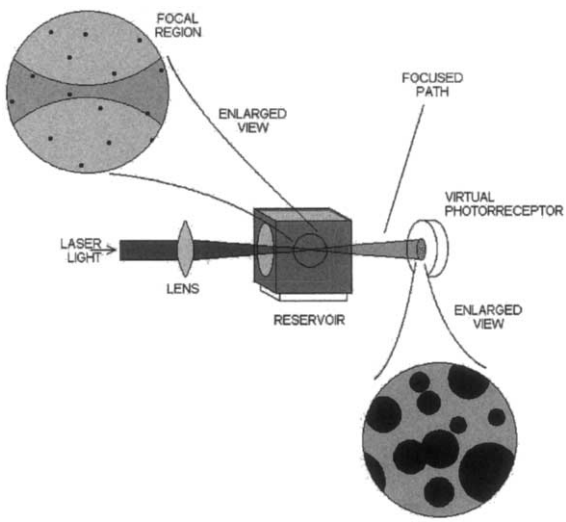

Fig. 1. Basic optical scheme used in the precipitation processes simulation program (PPSP).

$$\text{Transmittance} \equiv \frac{\text{Photorreceptor Area} - \text{Projected Area}}{\text{Photorreceptor Area}} \quad (1)$$

In the computational model, the noise associated with the transmittance has no sources other than those of the simulated experiment itself, so that noise sources such as those related to the measuring instruments, the imperfections of the experimental arrangement, changes in the experimental conditions, etc. are not included. Furthermore, if the factors that define the virtual beam path are kept constant, their influence may be considered constant throughout the simulated process.

However, the influence of the dynamic characteristics of the system, such as changes in position and orientation of the particles, blocking of the beam, etc. are very difficult to quantify. Out of this set of factors, the morphology of the precipitate might well be one of a significant influence, since the fluctuations in the transmittance that may be caused by changes in the position and orientation of the particles, depend on their morphology.

By way of example, let's imagine that an isolated spherical particle forms a precipitation system and that its centre of mass remains fixed at certain point of space. Let's also suppose that this particle can freely orientate itself, changing its orientation constantly and randomly.

If we could use a virtual photodetector to measure transmittances, we would obtain a stable signal due to the fact that the projected shadow does not change.

By contrast, if we analysed the influence of a flat particle in exactly the same conditions, we would find that its projection would show a great many variations, producing changes that would be recorded as noise associated with the transmittance.

Taking account of the definition of transmittance given by Eq. (1), if the averages of the areas projected during a given period of time in each of these two hypothetical precipitation systems coincided, it follows that the average transmittances should also coincide.

In such a case, the dispersion of the projected areas data from the mean area, would become a data describing the noise associated with the transmittance. The measure of dispersion we have opted for in order to obtain this information is the standard deviation.

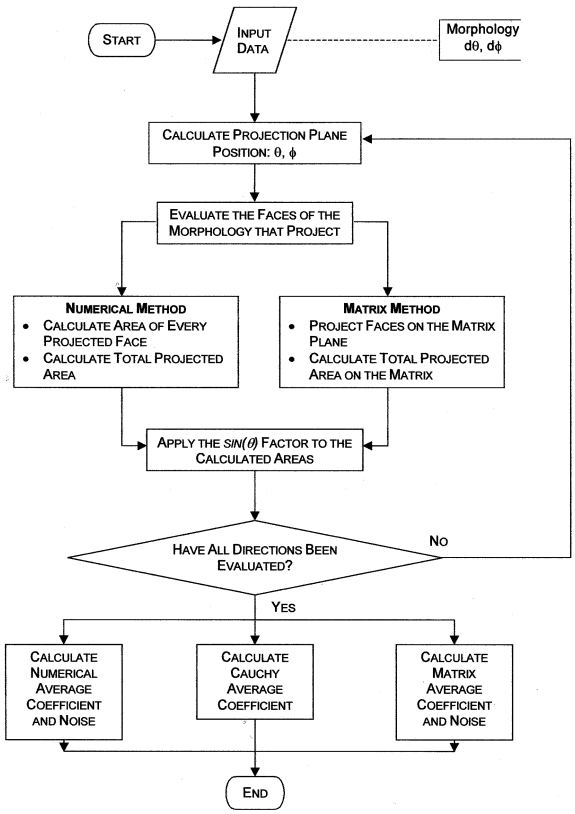

Fig. 2. Flow-chart of the program for the calculation of average coefficients and noises.

To make these calculations we have designed a computer program based upon the first of the two models presented above, i.e. the one with an isolated particle capable of randomly orientating itself. To fine-tune the program, it has been necessary to include the right algorithms that represent different morphologies in different spatial orientations and evaluates the projection areas on an orthogonal plane.

The program has been designed in FORTRAN[1] and the flow-chart describing how it works is shown in Fig. 2. The program applies two different methods to obtain noise data characteristic of every morphology: numerical and matrix calculation, both described in the following sections.

2.2. Numerical calculation of the noise

The morphologies analysed in this work are polyhedrons, i.e. volumes having all faces flat. Each face is mathematically represented by a normal vector. In order to calculate the area of the surface projected by a morphology with a given orientation, we need to know, first of all, which are the flat surfaces involved in the projection, and secondly, what is the contribution of each of these faces to the total projection.

To answer the first question we analyse the sign of each one of the scalar products of the normal vectors representing the volume's faces and the vector normal to the projection plane. All faces whose scalar product have the same sign (no matter what sign we choose), will be involved in the morphology's final projection, (Rogers, 1998).

Secondly, the total area of the surface projected by a morphology can be easily calculated through the following expression,

$$A = \sum_i S_i \cdot \cos \omega_i \tag{2}$$

where A is the area of the projection, S_i is the area of face i, and ω_i is the angle formed by the vector normal to face i and the vector normal to the projection plane.

The average projected area and the characteristic noise of the morphology are finally calculated as the arithmetic mean and standard deviation, respectively, of the areas of the projections thus generated.

2.3. Matrix calculation of the noise

The simulation of morphologies using the method based on matrix calculation takes place, generally speaking, in the same way as described in the previous section. The difference between these two methods lies in that once we know which faces of the morphology are involved in the global projection, we do not proceed with the numerical estimate of the area by using Eq. (2).

Instead, the morphology is projected on a bidimensional matrix (representing the photodetector), whose elements can contain numerical information. Those elements of the matrix on which there is no projection are given a value equal to zero (0), whereas the elements on which projection is detected, are given a value equal to one (1). Accordingly, the area of the projected surface may be calculated as the sum of all the elements in the matrix, as expressed in:

$$A = \sum_{j=1}^{n} X_j \tag{3}$$

where A is the area of projection, n is the total number of elements contained in the matrix on which projections take place, and X_j is the numerical value (0 or 1) assigned to the element j of the matrix.

The usefulness of the matrix method lies in two arguments: (a) it represents a method of calculation alternative to the numerical one, and (b) the algorithms used extend the possibilities of the PPSP.

[1] Microsoft Fortran Power Station. Copyright© 1993. Microsoft Corporation.

Indeed, the PPSP program (which simulates a precipitation process) evaluates a spherical particles multiple system, whereas the morphological noise calculation program analyses a system formed by one single particle. What both programs have in common is the fact that they use a matrix as a plane on which to evaluate the projections of the particles.

For that reason, if the results obtained through the matrix method are acceptably close to the numerical ones, the algorithms developed to represent morphologies will be validated and ready to be incorporated in the PPSP. In future studies the extended program may provide information concerning precipitation systems formed by non-spherical particles.

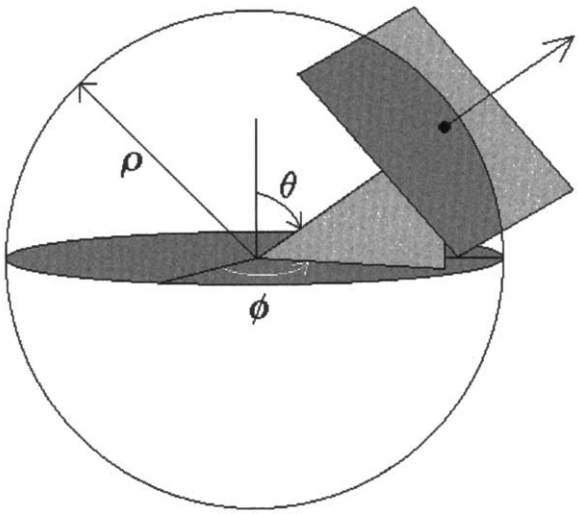

Fig. 3. Enveloping sphere used for calculating projected areas. The morphology to be studied must be placed at its geometrical centre. The projection plane varies its position according to the spherical coordinates, keeping a point of tangency with the surface of the enveloping sphere.

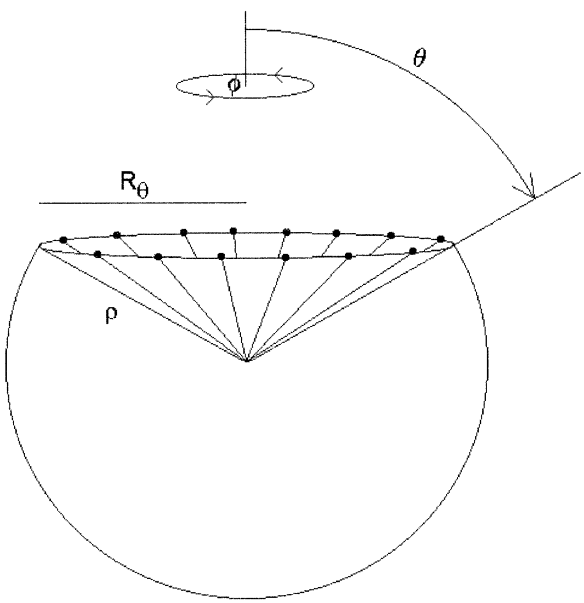

Fig. 4. The length of the circle generated by the cone of angle θ, has a radius R_θ, whose value is related to the radius of the enveloping sphere by means of the $\sin(\theta)$ factor.

2.4. Privileged orientations

In order to calculate the average area of the projected surfaces and the noise associated with each morphology using both the numerical and matrix methods, it is necessary to know some data on surface projected by the morphologies in different spatial orientations.

Computationally, the collection of these data has been based on the following considerations:

1. The morphology to be analysed remains stationary at the centre of an enveloping sphere of radius ρ.
2. The mobile plane on which the projection is mapped takes positions tangent to the enveloping sphere.
3. The spatial orientations to be evaluated are expressed in angular spherical coordinates ($\theta\, y\, \phi$), which correspond with the direction defined by the radius vector with origin at the centre of the enveloping sphere and ending at the point of tangency between the sphere and the projection plane. These coordinates coincide with those of the vector normal to the projection plane shown in Fig. 3.

In this model, each (θ, ϕ) pair represents a different spatial orientation of the analysed morphology. The coordinate θ varies between 0 and 180°, whereas ϕ varies between 0 and 360°. If the radius vector moved along the surface of the enveloping sphere changing its coordinate ϕ at a rate of constant angular intervals, and we traced its directions by means of a straight line with origin at the centre of the enveloping sphere, we would obtain a situation equivalent to the one shown in Fig. 4.

It can be seen from Fig. 4 that for each value of θ, the radius vector describes a cone that envelops the directions defined by ϕ. Each one of these cones intersects with the enveloping sphere forming a circumference whose length depends on θ. The value of the length is maximum in the direction given by $\theta = 90°$, and null in those given by $\theta = 0$ and 180°.

If for every direction θ we analysed an equal number of directions ϕ, represented as dots on the enveloping sphere, we would find that the final distributions of these dots would not be uniform. It would be more concentrated at the poles ($\theta = 0$ or 180°) and more scattered at the equator ($\theta = 90°$).

If the calculations were made analysing this distribution of directions, the results would be strongly influenced by the concentration of directions at polar

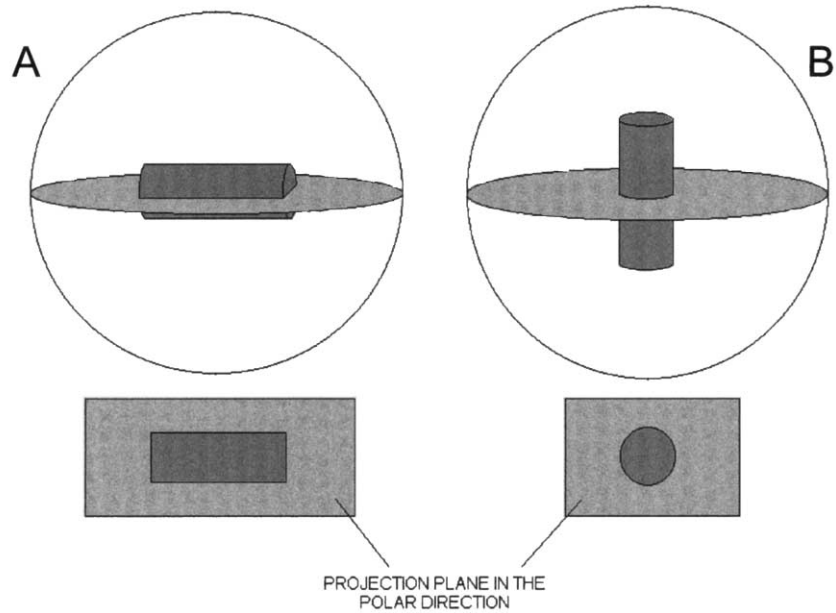

Fig. 5. This figure shows the surface projected by a cylinder placed at the centre of the enveloping sphere in different orientations. In figure (A), the projected surface on the polar direction is a rectangle. In figure (B), it is a circle. If the influence of the privileged orientations were not considered, the average coefficients would be different in both cases.

regions. The final result, therefore, would depend on the initial orientation of the morphology studied (Fig. 5).

Solving this problem requires that the distribution of dots representing directions, have a uniform density on the surface of the enveloping area.

To that end, it is only necessary that the number of directions ϕ to be evaluated for every value of θ, be proportional to the length of the circumference of radius R_θ, and therefore,

No. of directions ϕ in the orientation $\theta = N_\theta$

$$N_\theta \propto L_\theta$$

$$N_\theta \propto 2\pi R_\theta = 2\pi\rho \sin(\theta)$$

$$N_\theta \propto \sin(\theta) \tag{4}$$

where L_θ is the length of the circumference of radius R_θ, and ρ is the radius of the sphere enveloping the morphology.

That is to say, in order to obtain a set of uniform spatial directions, we should select, for every angle θ, a number of directions ϕ proportional to $\sin(\theta)$.

An equivalent methodology consists of evaluating a constant number of directions ϕ for every value of θ but weighing the results with the $\sin(\theta)$ factor.

2.5. Description of the morphologies analysed

The mathematical and computational description of the 32 crystallographic groups (Vainshtein, 1994) is an arduous, time-consuming task. For that reason we have made a selection of morphology types which includes three-, four- and six-sided faces polyhedral prisms, called in this work P3, P4 and P6, respectively.

These morphologies have been analysed in a whole variety of lengths ranging from 0.25 to 3.0 times the length of the main edge. It has also been included a special length of 0.1 to emulate a quasi-flat morphology.

Other morphologies derived from those mentioned above by adding three-, four- and six-sided pyramids have also been analysed. These morphologies, which we called P3P, P4P and P6P have been analysed using the same size relationship as with P3, P4 and P6, although incorporating a 0.0 length factor, corresponding to the non-prismatic bipyramidal varieties. A graphic representation of these morphologies, together with the main edge for every one of them, is shown in Fig. 6.

The pyramids added to prisms P3P and P4P are formed by equilateral triangles whose side lengths are equal to the main edge. However, that is not possible in the case of the 6-sided polyhedron, since the bases on which the six-sided pyramids are placed are regular

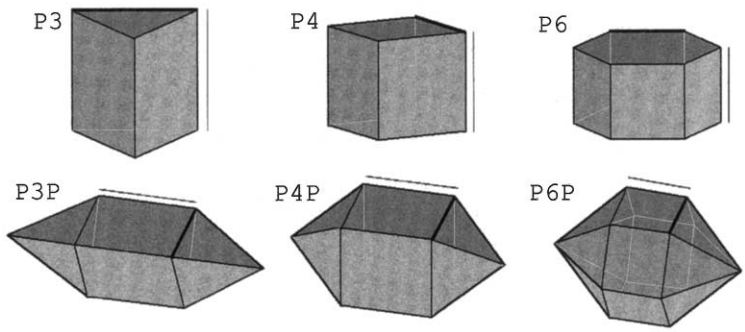

Fig. 6. Description of morphologies. Every volume shows a thicker line, which indicates the principal edge. A line has been drawn next to each morphology, to show the edge that defines the length of the volume. This may be from 0.0 to 3.0 times the length of the principal edge. In this figure, only 1.0 lengths have been drawn.

hexagons, and the only possible disposition of equilateral triangles on such a base would have to be on the same plane. In this case, the height of the pyramid has been arbitrarily assigned a value equal to the length of the main edge.

2.6. Election of comparable volumes

In the analysis of morphologies there is clearly a relationship between noise, interpreted as the standard deviation of the projected areas from their mean value, and the size of the morphology. The larger the volume, the larger the projected surfaces and the higher the absolute values of the variations caused by changes in the orientation.

For that reason, in order to analyse the morphological noise in terms of standard deviation, it is necessary to set a criterion that eliminates the influence of size.

To establish this criterion we will return to the one single isolated particle system. The particle changes its orientation continuously and randomly, and the average transmittance of the system is a data equivalent to that of the average projected area. If we compare morphologies whose average projections coincide, we are comparing virtual systems with equal levels of transmittance and with comparable associated noises.

Therefore, comparable volumes are those which project the same average areas, which are easily obtained using Cauchy's theorem (Cauchy, 1908; Van De Hulst, 1981; Brown and Felton, 1985; Hostomský et al., 1986).

According to this theorem, the average area projected by a convex volume[2] that changes its orientation randomly can be calculated as one fourth of the surface enveloping it, that is:

Average Projected Area ($\overline{A}$)

$$= \frac{\int_{-\pi}^{\pi}\int_{0}^{\pi} f(\theta,\phi)\,\sin(\theta)\mathrm{d}\theta\,\mathrm{d}\phi}{\int_{-\pi}^{\pi}\int_{0}^{\pi} \sin(\theta)\mathrm{d}\theta\,\mathrm{d}\phi} = \frac{S}{4} \tag{5}$$

where $\sin(\theta)\,\mathrm{d}\theta\,\mathrm{d}\phi$ represents the surface differential element of a sphere of radius 1, θ and ϕ are the coordinates that define the direction of the vector normal to the projection plane, $f(\theta, \phi)$ is the function that gives the area of the projection of the morphology on an orthogonal plane whose normal vector is in the direction defined by (θ, ϕ), and S represents the enveloping surface of the convex volume analysed.

Therefore, Cauchy's average represents an important reference inasmuch as the application of the computational model used in this work does not include the infinite number of possible orientations which, on the contrary, Cauchy's theorem does evaluate.

In order to derive the expressions that give comparable volumes, it is necessary to combine the expressions describing the volume of each morphology, with the ones that give Cauchy's average area.

Table 1 shows the analytical expressions describing the calculation of comparable volumes whose average projections generate the same average area, $\overline{A}$. The Cauchy average coefficient has also been included, a non-dimensional value obtained by dividing the average projected surface (Cauchy average area) by the square of the length of the main edge (a^2). Thus defined, this value will characterise the morphology regardless of its size.

3. Results and discussion

The volumes analysed correspond to those generated by an average projected surface of 1000 arbitrary units. These volumes have been estimated by substituting the

[2] A volume that is intersected only at two points by a straight line passing through it in any direction.

Table 1
Analytical equations for the calculation of the volume for the different morphologies are listed

Morphology	Volume	Cauchy average area $(\bar{A}) = S/4$	Cauchy average coefficient	Volume of comparable morphologies
P3	$\frac{\sqrt{3}}{4}La^3$	$\left(\frac{\sqrt{3}}{2}+3L\right)\frac{a^2}{4}$	$\frac{\sqrt{3}}{8}+\frac{3}{4}L$	$\frac{\sqrt{3}}{4}L\left(\frac{4\bar{A}}{\frac{\sqrt{3}}{2}+3L}\right)^{3/2}$
P3P	$\left(\frac{1}{3\sqrt{2}}+\frac{\sqrt{3}}{4}L\right)a^3$	$\left(3\frac{\sqrt{3}}{2}+3L\right)\frac{a^2}{4}$	$\frac{3\sqrt{3}}{8}+\frac{3}{4}L$	$\left(\frac{1}{3\sqrt{2}}+\frac{\sqrt{3}}{4}L\right)\left(\frac{4\bar{A}}{3\frac{\sqrt{3}}{2}+3L}\right)^{3/2}$
P4	La^3	$(2+4L)\frac{a^2}{4}$	$\frac{1}{2}+L$	$L\left(\frac{4\bar{A}}{2+4L}\right)^{3/2}$
P4P	$\left(\frac{\sqrt{2}}{3}+L\right)a^3$	$(2\sqrt{3}+4L)\frac{a^2}{4}$	$\frac{\sqrt{3}}{2}+L$	$\left(\frac{\sqrt{2}}{3}+L\right)\left(\frac{4\bar{A}}{2\sqrt{3}+4L}\right)^{3/2}$
P6	$\frac{3\sqrt{3}}{2}La^3$	$(3\sqrt{3}+6L)\frac{a^2}{4}$	$\frac{3\sqrt{3}}{4}+\frac{6}{4}L$	$\left(\frac{3\sqrt{3}}{2}L\right)\left(\frac{4\bar{A}}{3\sqrt{3}+6L}\right)^{3/2}$
P6P	$\left(\sqrt{3}+\frac{3\sqrt{3}}{2}L\right)a^3$	$(3\sqrt{7}+6L)\frac{a^2}{4}$	$\frac{3\sqrt{7}}{4}+\frac{6}{4}L$	$\left(\sqrt{3}+\frac{3\sqrt{3}}{2}L\right)\left(\frac{4\bar{A}}{3\sqrt{7}+6L}\right)^{3/2}$

The Cauchy averaged area is listed as well, in terms of the length factor (L), together with the analytical expressions of comparable volumes and the Cauchy average coefficients.

corresponding length factors (L) and the value $\bar{A} = 1000$, in the 'volume of comparable morphologies' column in Table 1.

The variations of the average coefficients calculated is shown in Fig. 7,

1. by applying Cauchy's theorem;
2. by applying the computer program using the numerical method;
3. by applying the computer program using the matrix method.

The coefficients computationally obtained (b and c) were calculated by evaluating the directions defined by the angular coordinates θ and ϕ, varying from 0 to 180°, with an angular interval of 0.5°.

It can be seen from the graphs in Fig. 7 that the average coefficients are very close, regardless of the method of calculation used. This indicates that the directions evaluated constitute a subset representative of the infinite number of possibilities. Furthermore, they validate the computational algorithms designed to represent each morphology.

The matrix coefficients are optimally close to the numerical ones. However, they present a higher deviation from the Cauchy coefficients. This discrepancy may be accounted for by rounding-off errors made when projecting volumes (defined in the field of real numbers) on the matrix plane (defined in the field of integer numbers[3]). The graphs show that the deviation of the coefficients increases as the value of the length parameter (L) is higher. This is due to the fact that the rounding-off problems are concentrated around the perimeter of the projected surfaces.

In the projection of elongated volumes, the contribution of the perimeter to the total projection is quantitatively larger than that of volumes with more symmetrical proportions[4]. As a consequence, the higher

[3] To minimise these discrepancies we would simply have to use a matrix plane with a larger number of elements. Increasing the resolution would demand more memory and would entail slowing down the calculation program.

[4] For example, a 2×2 square has an area of 4 units and a perimeter of 8. A 1×4 rectangle has exactly the same area but it has a perimeter of 10 units.

the value of the length parameter (L), the likelier the morphologies are to make rounding-off errors and the more different will be the matrix coefficients from the numerical ones.

The data on noise associated with the morphologies, calculated by applying the computer program using the numerical and matrix methods are shown in Fig. 8. These graphs also show the evolution of the Ψ function, defined as the quotient between the volume of an equivalent sphere and the volume of the morphology analysed.

Given that they are all convex volumes, and we can apply Cauchy's theorem to them, all the morphologies studied have in common the area of the enveloping surface, $S = 4 \cdot \bar{A} = 4000$ surface units.

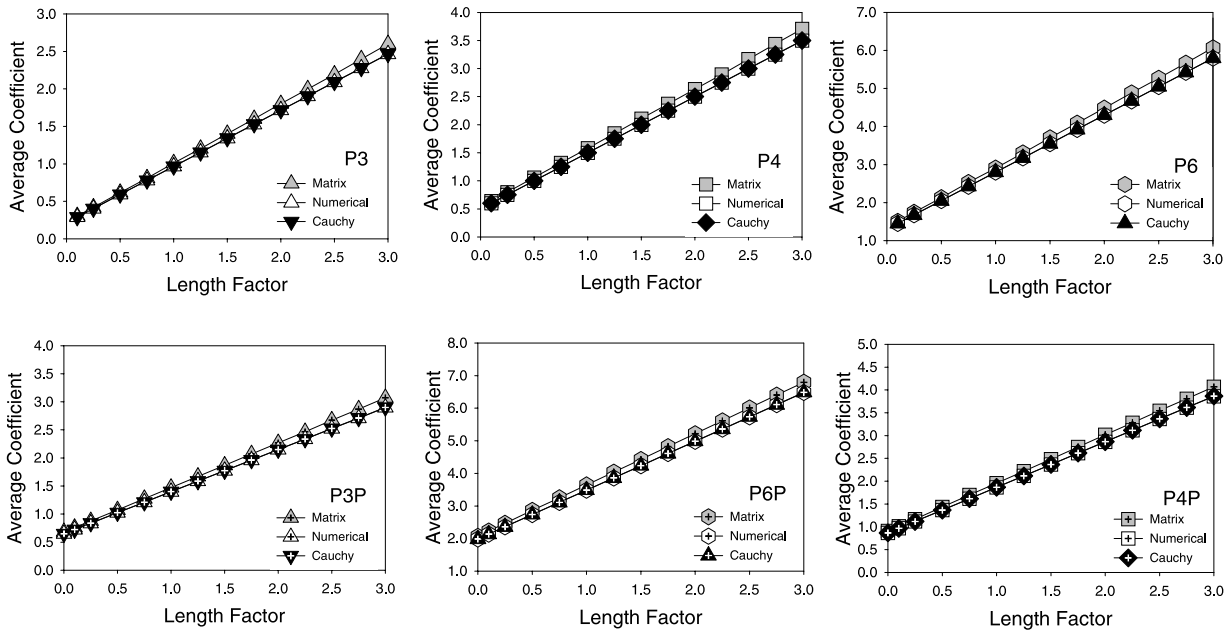

Fig. 7. Average coefficients calculated by the matrix, numerical and Cauchy methods. The graphs show length factors versus average coefficients.

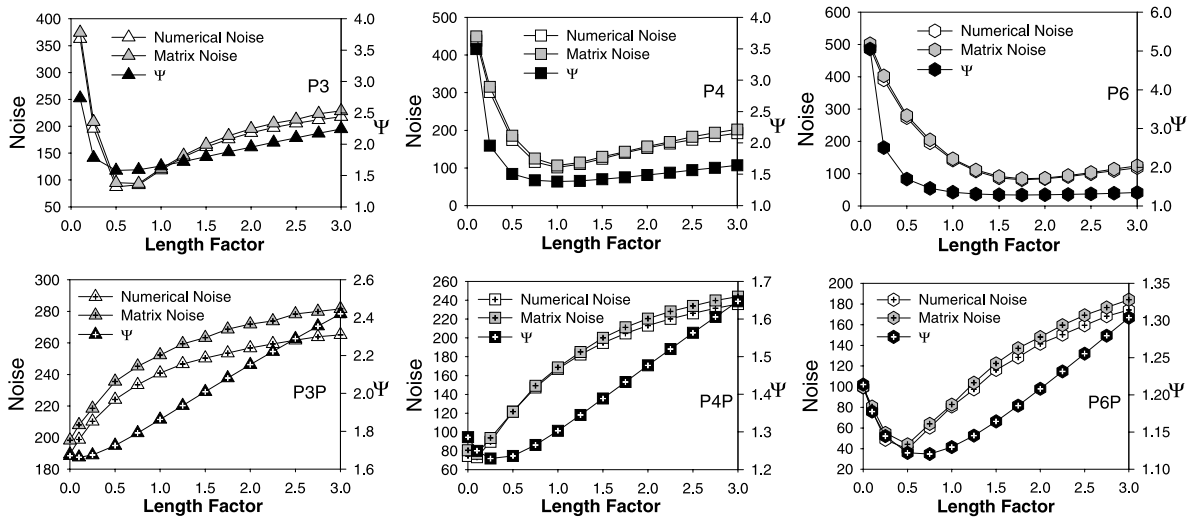

Fig. 8. Variations of the numerical and matrix noise and of the Ψ function, for every morphology. The graphs show length factors versus noises and the Ψ function.

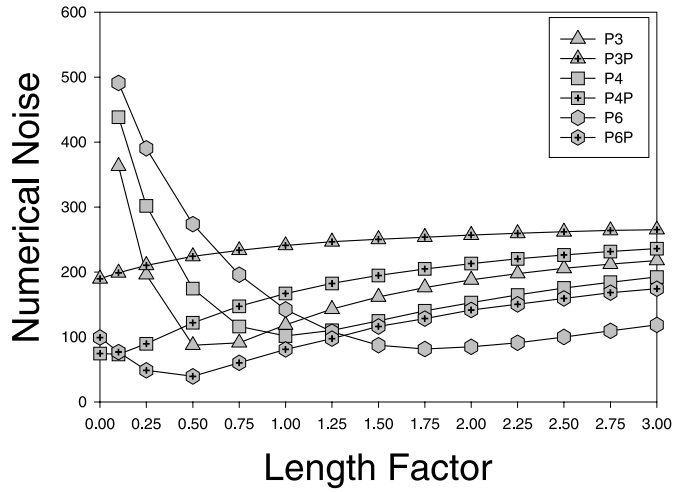

Fig. 9. Morphology classification in terms of the numerical noise.

In these circumstances, the sphere is the morphology that has a volume maximum, and for that reason, the Ψ function represents, by means of a non-dimensional factor, the level of morphological analogy with the sphere in volumetric terms. Furthermore, the sphere is the only morphology whose level of noise is null, and because of that, the variation of the Ψ function related to the value of L, provides information concerning the level of morphological noise.

As we can see from Fig. 8, the plotting of the Ψ function is very similar to that of the noise data. Therefore, Ψ becomes an important argument that accounts for the relation of morphological noise as a consequence of volumetric resemblance to the equivalent sphere.

However, although the plotting of these functions share some similarities, there are some clear differences too. This suggests that the noise, in addition, establishes a dependence related to how the enveloping surface is located in space.

The graph in Fig. 9 shows the different levels of numerical noise for every morphology. It allows us to clearly discern the relative classification of morphologies in terms of noise for every value of the length factor (L).

It can be seen that the quasi-flat morphologies (P3, P4 and P6 with $L = 0.1$), represent higher levels of noise. In addition, the more edges in the polyhedron, the higher the level of noise.

From Fig. 9 we can infer that there is clearly a relationship between noise and length of the morphology. As the length increases, the levels of noise tend to get closer to one another. In the hypothetical limit for which L would have a value similar to infinite, all the morphologies tend to have elongated, similar structures. In that case we should expect to find identical levels of noise for every morphology.

4. Conclusions

The study of the level of noise associated with a morphology is based on the isolated analysis of the particle to be studied and on the calculation of areas projected on an orthogonal plane.

Different morphologies may be compared when the volumes used are those that generate the same average transmittance, whose noise is exclusively caused by morphological factors.

The level of morphological noise can be approached through the Ψ factor, which describes each morphology in terms of volumetrical resemblance to the equivalent sphere. However there is another factor of influence given by the spatial disposition of the enveloping surface of every morphology.

The theoretical results obtained confirm the validity of the hypothesis set forth in the experimental work (Poce-Fatou et al., 2001a). In that work it was detected that the level of noise associated with the transmittance was higher in the case of flat particles of PbI_2 and $PbSO_4$ and clearly lower in the case of elongated particles of $BaSO_4$ and BaC_2O_4.

Acknowledgements

This work was supported by the Spanish DGICYT under grant ALI97-0885.

References

Brown, D.J., Felton, P.G., 1985. Chem. Eng. Res. Des. 63, 125.

Cauchy, A., 1908. Oevres Complétes d'Augustin Cauchy, vol. II, 1st ed. Gauthier-Villars, Paris.

Gerrard, A., Burch, J.M., 1994. Introduction to Matrix Methods in Optics. Dover Publications, New York.

Hostomský, J., Halász, Z., Liszi, I., Nývlt, J., 1986. Powder Technol. 49, 45–51.

Martín, J., Alcántara, R., García-Ruiz, J.M., 1991. Cryst. Res. Technol. 26, 35.

Martín, J., García-Ruiz, J.M., Alcántara, R., 1992. Cryst. Res. Technol. 27, 799.

Poce-Fatou, J.A., Alcántara, R., Gallardo, J.J., Martín, J., 2001a. Comput. Chem., in press.

Poce-Fatou, J.A., Alcántara, R., Martín, J., 2001b. Comput. Chem., in press.

Rogers, D.F., 1998. Procedural Elements for Computer Graphics, 2nd ed. WCB/McGraw-Hill, New York.

Vainshtein, B.K., 1994. Fundamentals of Crystals. Springer-Verlag, Berlin.

Van De Hulst, H.C., 1981. Light Scattering by Small Particles. Dover Publications, New York.